Journal of Mines, Metals and Fuels, *71(9): 1336-1345; 2023. DOI: 10.18311/jmmf/2023/35459*

Print ISSN : 0022-2755

Journal of Mines, Metals and Fuels

Contents available at: *www.informaticsjournals.com/index.php/jmmf*

Effect of Strain Per Pass on Microstructure and Mechanical Properties of Multi-Axially Forged Cast AA5083 Alloy at Room Temperature

Gajula Aravindh*, G. V. Preetham Kumar and K. Udaya Bhat

Department of Metallurgical and Materials Engineering, National Institute of Technology, Karnataka, Surathkal – 575025, India; gajula.aravindh@gmail.com

Abstract

This paper investigates the effect of strain per pass over a cycle on, multi-axially forged cast AA5083 alloy at room temperature. To begin with, Multi-Axial Forging (MAF) with two different strains per pass was imposed on the alloy without changing the die geometry. Samples were deformed to cumulative strains of Σε = 2.46 (2 Cycles) and Σε = 2.79 (3 Cycles), with two different strains per pass ε = 0.41 and ε = 0.31 respectively. Microstructural analysis was carried out by using OM, XRD, and SEM with EDS. Structural changes were characterized, and it was revealed that grain fragmentation was caused by the frequent development of deformation and micro shear bands, which was followed by the evolution of new fine grains in the original grain structure. Mechanical properties were evaluated by tensile, and hardness tests. MAF of ε = 0.41 per pass results in high tensile strength and hardness, 428 MPa and 147 Hv; respectively at a cumulative strain of Σε =2.46. Processing with strain ε = 0.31 per pass produced strength of 380 MPa and hardness of 131 HV after cycle III with a cumulative strain of 2.79. MAF of strain ε = 0.41 per pass with cumulative strain of 2.46 resulted in a higher grain refinement structure with increased strength compared to a strain of 0.31 per pass with a cumulative strain of 2.79. Therefore, with the imposition of the high strain per pass produced more grain refinement and consequently higher strength.

Keywords: *Cast AA 5083alloy, Grain Refinement, Multi Axial Forging, Strain Per Pass*

1.0 Introduction

Al-Mg alloys are extensively used in structural applications in the transportation sector in the field of automotive, aerospace, and marine engineering due to the excellent combination of high strength-to-weight ratio, good formability, high toughness, excellent weldability, and corrosion resistance[1]. These alloys belong to the 5XXX series of non-heat-treatable Al alloys, and their strength is mostly derived from solid solution strengthening via Mg solute content. Mg is restricted despite its higher solubility in the Al matrix. Al alloys with Mg content beyond 3.5 wt.%, when subjected to moderately high temperatures (60-180 °C), are likely to experience Stress Corrosion Cracking (SCC) and Intergranular Corrosion (IGC)[2,3]. Phase formation, namely Al_3Mg_2 along the grain boundaries is majorly responsible for the SCC and intergranular corrosion above 65 °C[4]. The main limitation of these alloys is their low strength. AA5083 alloy is in the family of 5XXX Al alloys and offers the highest strength among the non-heat treatable A1 alloys. Due to the lower strength of their alloys applications in the industry are limited. To widen applications, strength of these alloys is to be increased. These alloys could be further strengthened through work hardening and grain refinement.

Severe Plastic Deformation (SPD) is very attractive to material scientists in modern days due to the enhancement of the material properties, especially strength by grain

**Author for correspondence*

refinement without changing the dimensions of the material[5]. SPD methods, such as Equal Channel Angular Pressing (ECAP)[6,7], High-Pressure Torsion (HPT)[8,9], Accumulative Roll Bonding (ARB)[10], Multiaxial Forging (MAF)[11,12], twist extrusion[13] etc., are popular.

Among all SPD methods, multiaxial forging is getting more attention due to ease of operation and this method can be scaled up to small and medium-scale components. The main advantage of MAF processing is strain imposition. Strain is independent of die geometry. In this method, we can impose a high amount of strain per pass by changing the sample dimensions without changing the die geometry, unlike ECAP, HPT, and other SPD processes. MAF is characterized by plane strain deformation, which is accomplished by compressing the workpiece through a split die. The sample is pressed to a fixed strain in the die, then removed and rotated by 90°, reinserted into the die, and the process is repeated in all three mutually perpendicular directions. MAF die assembly, top-view representation, and schematic representation of the MAF procedure is shown in Figure 1[14].

The MAF process is done completely under plane strain conditions, in which one of the principal strains is equal to zero ($\varepsilon_2 = 0$). According to 'Von mises' criteria, effective strain (ε_{eff}) can be evaluated by using Equation 1.

$$\varepsilon_{eff} = \left[\frac{2}{3}(\varepsilon_1^2 + \varepsilon_2^2 + \varepsilon_3^2)\right]^{\frac{1}{2}} \quad \textbf{(1)}$$

$$\varepsilon_{eff} = \left[\frac{2}{3}(\varepsilon_1^2 + 0 + \varepsilon_3^2)\right]^{\frac{1}{2}} \quad (\text{where } \varepsilon_2 = 0)$$

$$\varepsilon_1 + \varepsilon_2 + \varepsilon_3 = 0;\ \varepsilon_1 = -\varepsilon_3$$

$$\varepsilon_{eff} = \left[\frac{2}{3}(2 * \varepsilon_1^2)\right]^{\frac{1}{2}}$$

$$\varepsilon_{eff} = \frac{2}{\sqrt{3}}\varepsilon_1 \quad \text{where } \varepsilon_1 \text{ is the true strain}$$

$$(\varepsilon_1 = \ln(\frac{hi}{h_f}))$$

It has been shown recently that such strain accumulation becomes very important to achieve the homogeneous microstructures of equiaxed grains separated by high angle grain boundaries[15]. However, grain refinement during interrupted deformation may be controlled not only by total strain accumulated but also by strain per each pass[16]. Strain imposition in the

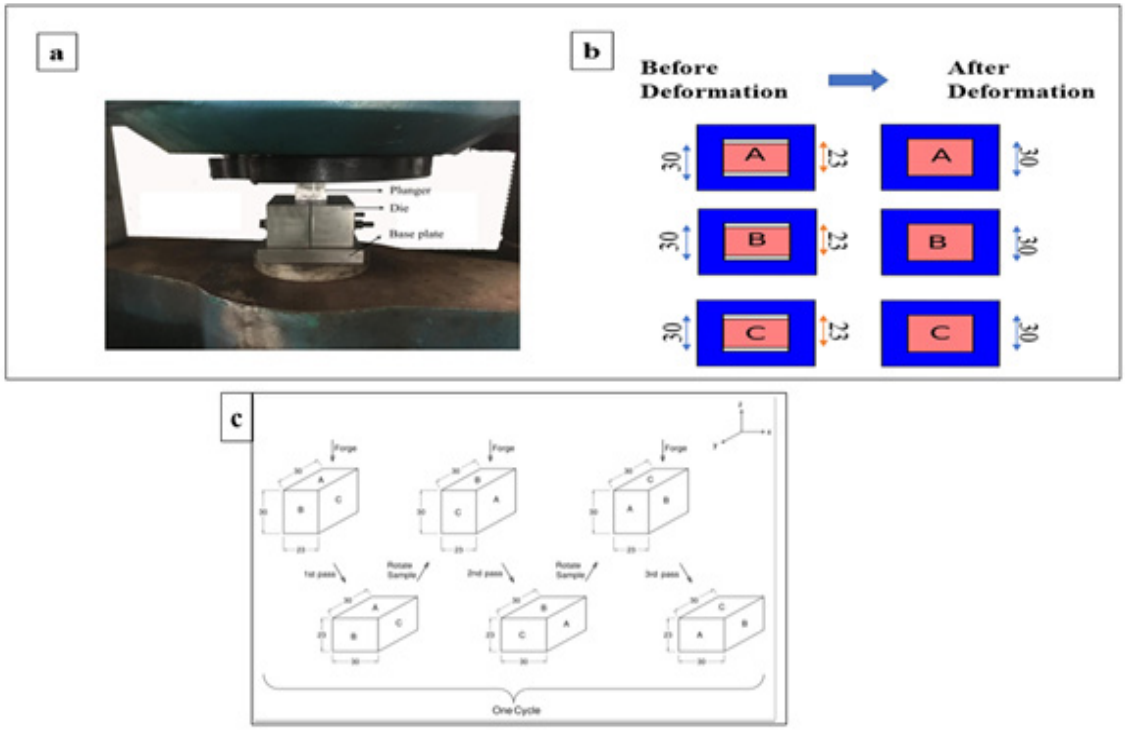


Figure 1. MAF process **(a)** MAF die assembly, **(b)** Top view, **(c)** Schematic representation.

material is independent of the die geometry. So, it is important to know the effect of strain per pass during the process. Sitdikov *et al.*[17] reported the effect of strain per pass on Al7475 alloy at higher temperatures. It is equally important to know this effect at room temperature. As of now, no literature reported the effect of strain per pass on AA5083 alloy.

In current work, the effect of strain per pass in the Al-Mg alloys (AA5083) processed through multi axial forging was studied at room temperature.

2.0 Experimental Procedure

Commercial AA5083 alloy was used and the chemical composition is mentioned in Table 1. AA5083 alloy ingots were remelted at 750 °C, using a SiC crucible in an electric furnace. After reaching the temperature, the melt was degassed with hexachloroethane tablets. 'Coverall AR' covering flux was added to the melt to prevent surface oxidation, and any dross on the surface was scraped off. The melt was stirred with a graphite rod and the dross, if any was skimmed off further. The melt was poured into the preheated mold. The material was cast into ingots bar of length and width of 120x32 mm.

The cast ingot was homogenized at 450 °C for 5h followed by water cooling to ambient temperature, to relieve the internal stress generated during the casting. Homogenized samples were machined to two different geometries, such as 30x30x23 mm and 30x30x21 mm and these samples were subjected to MAF processing. MAF die was made by using H11 tool steel. The MAF process was done using a 200-ton capacity UTM with a constant pressing speed of 0.5 mm/minute. Two different levels of strains (0.31 and 0.41 strains per pass) were imposed on the sample according to Equation 1. Cumulative strain imposed on the sample was calculated according to the Equation 2[18].

$$\varepsilon_{cumulative} = \frac{2}{\sqrt{3}} * n * \ln\left(\frac{h_i}{h_f}\right) \quad (2)$$

where, n is the number of passes, h_i and h_f are the initial and final height of the sample.The alloy was subjected to 3 cycles with 0.31 strain per pass and 2 cycles with 0.41 strain per pass.

For microstructural analysis, the mid-section of the sample perpendicular to the last forging pass was taken from the sample. Microstructural investigation was done by using Optical Microscopy (OM), Field Emission Scanning Electron Microscopy (FESEM-7610FEPLUS, JEOL, JAPAN) equipped with an attachment for Energy Dispersion Analysis (EDS). These samples were subjected to mechanical polishing and then modified poultan etchant (12 ml HCl, 30 ml HNO_3, 1 ml HF, 40 ml H_2O, and 4g chromic acid) for 10s. X-Ray Diffractometry (XRD, Empyrean 3rd Gen, Malvern Panalytical, Netherlands) profile was generated using a computer-controlled diffractometer with Ni filter operated at 30kV and 20mA with Cu-k_α radiation with a diffraction angle (2θ) ranging from 10° to 90° and at a scanning speed of 6° per minute. Mechanical tests, such as tensile tests were done using a 100 kN AG–X plus™ Shimadzu universal testing machine. Tensile tests were prepared according to the ASTM E8 standard with dimensions, such as 4 mm gauge diameter and 16 mm gauge length and were carried out with a ram speed of 0.5 mm per minute at room temperature. Hardness of the samples was evaluated by using Shimadzu Vickers micro-hardness tester. For Vickers microhardness, polished samples were subjected to a 200g load with a dwell period of 15s. For each sample average of 10 readings were considered.

3.0 Results and Discussion

AA5083 alloy was successfully forged with different strains per pass, such as ε = 0.31 and ε = 0.41 at room

Table 1. Chemical composition of the AA5083 alloy (in wt.%)

Mg	Mn	Si	Fe	Cr	Cu	Zn	Ti	Al
4.33	0.433	0.127	0.189	0.228	0.016	0.0084	0.002	94.60

temperature for 3 cycles (Σε = 2.79) and 2 cycles (Σε = 2.46), respectively.

3.1 XRD Analysis

X-ray diffraction patterns of the as-cast, homogenized, and MAF processed with different strains per pass are shown in Figure 2. Plots (a) and (b) in Figure 2, show the as-cast and homogenized samples of AA5083 alloy. Plot c-e and f-g represents the MAF-processed AA5083 alloy with two different strains per pass 0.31 and 0.41 respectively. Face-centered cubic α Al phase is detected in all the samples despite the presence of Mg more than 4 wt.%. This is attributed to the low decomposition rate of Mg in Al-Mg alloys, which has been reported in the literature[19,20].

In as cast alloy, peak intensity is maximum along (311). After homogenization intensity was observed maximum corresponds to the (111) plane. Further, processing with MAF strain, the intensity of the plane (111) was slightly reduced up to 'e' plot with 0.31 strain per pass and also from 'f' to 'g' plot with 0.41 strain per pass, subsequently increased along the (200), (211), (3111) and (222) planes. Reducing the intensity of the (111) plane is due to the grain refinement and weakening of texture. Also, with the imposition of the strain, peak broadening was increased which defines the reduction in the grain size and also observed that the peak intensity shifted from (111) plane to (200) and (220). These are attributed to grain refinement and increasing dislocation density of the material[21].

3.2. Microstructural Investigations

Microstructural characterization was analyzed by optical microscopy and FESEM. The optical microstructure of the as-cast, homogenized, and MAF-processed samples with different strain per pass is shown in Figure 3. Microstructure of the as-cast alloy and homogenized AA5083 alloy shown.

In Figure 3 (a) and (b) respectively. MAF processed AA5083 alloy with 0.31 strain per pass I, II, and III cycles were shown in Figure 3 (c), (d), and (e) respectively. MAF process with 0.41 strain per pass I and II cycle is shown in Figure 3 (f) and (g) respectively. Microstructure of the as-cast alloy consists of a dendritic structure with an average grain size of about 732 µm. The grain size of

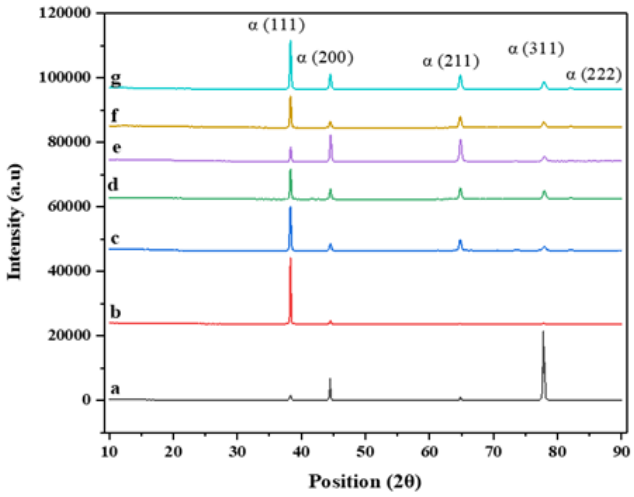


Figure 2. XRD profile of AA5083 alloy subjected to MAF processes with different strain per pass **(a)** as cast, **(b)** homogenized, **(c)** I cycle (0.31 strain per pass), **(d)** II cycle (0.31 strain per pass), **(e)** III cycle (0.31 strain per pass), **(f)** I cycle (0.41 strain per pass), **(g)** II cycle (0.41 strain per pass).

the homogenized sample was slightly reduced to 561 µm. MAF processed sample with 0.31 strain per pass after 1st cycle, the dendritic structure was broken and grain refinement was started and the grain size of the alloy was reduced to 350 µm. With further imposition of the strain, grain boundaries vanished. After 2nd and 3rd cycles, micro shear bands and deformation bands were formed in the alloy's microstructure. MAF processed sample with 0.41 strain per pass after 1st cycle, grain size was reduced to 148 µm. Grains were broken with further imposition of the strain. After the 2nd cycle, the material's grain size was further reduced to 125µm. With high imposition strain per pass has refined the grain size by 73% compared to the 0.31 strain per pass which reduced by around 29%.

SEM micrographs of AA5083 alloy, under as cast, homogenized and subjected to MAF with 0.31 and 0.41 strain per pass are shown in Figure 4. As-cast microstructure consists of dendrites as shown in Figure 4(a). After homogenization, secondary precipitates were formed and identified as $Al_6(Fe,Mn)$ and Mg_2Si[22]. With the increase in strain, secondary precipitates were broken and distributed evenly throughout the sample. After 3 cycles of MAF with 0.31 strain per pass secondary precipitates were distributed evenly in the sample as shown in Figure

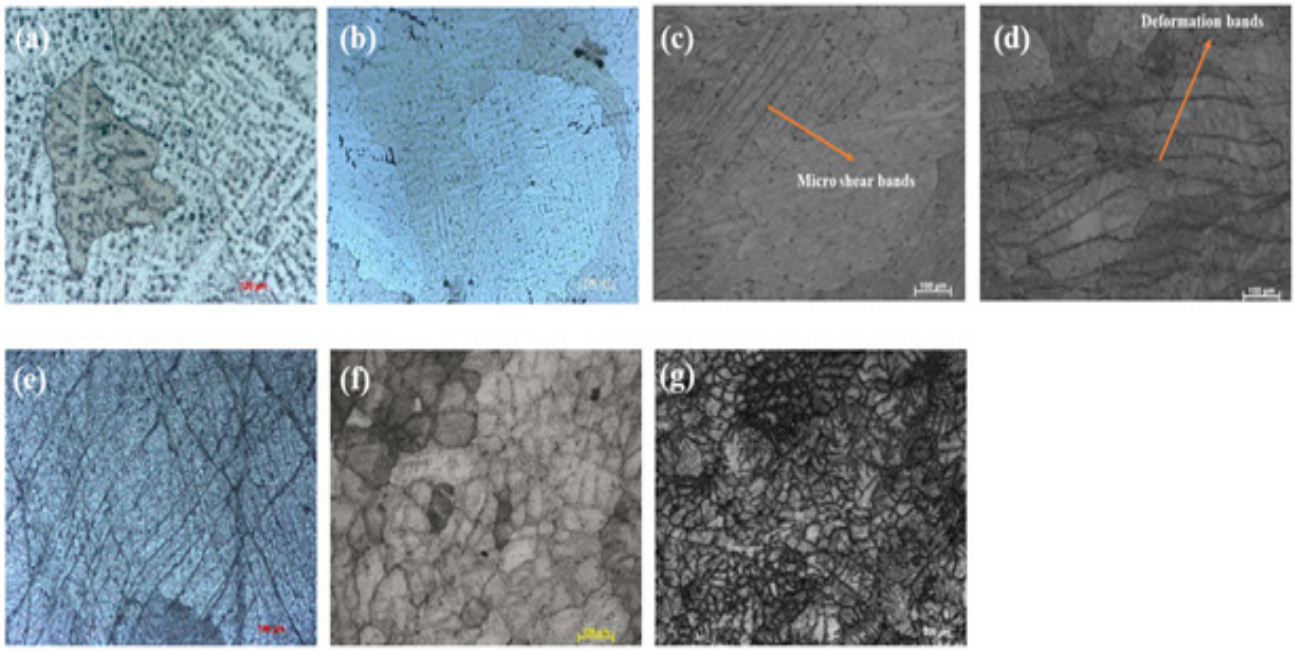


Figure 3. Optical microstructures of the AA5083 alloy subjected to different processing conditions **(a)** as cast, **(b)** homogenized, **(c)** I cycle (0.31 strain per pass), **(d)** II cycle (0.31 strain per pass), **(e)** III cycle (0.31 strain per pass), **(f)** I cycle (0.41 strain per pass), **(g)** II cycle (0.41 strain per pass).

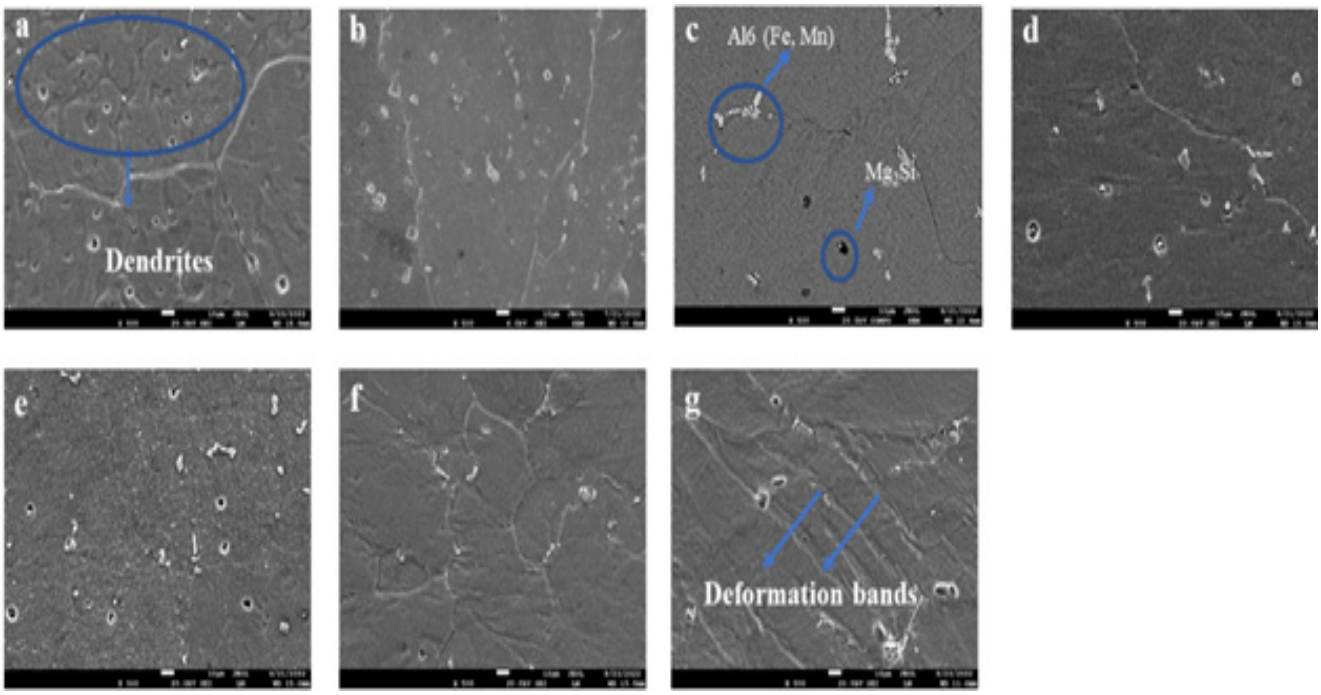


Figure 4. SEM images of AA5083 alloy **(a)** as cast, **(b)** homogenized, **(c)** I cycle (0.31 strain per pass), **(d)** II cycle (0.31 strain per pass), **(e)** III cycle (0.31 strain per pass), **(f)** I cycle (0.41 strain per pass), **(g)** II cycle (0.41 strain per pass).

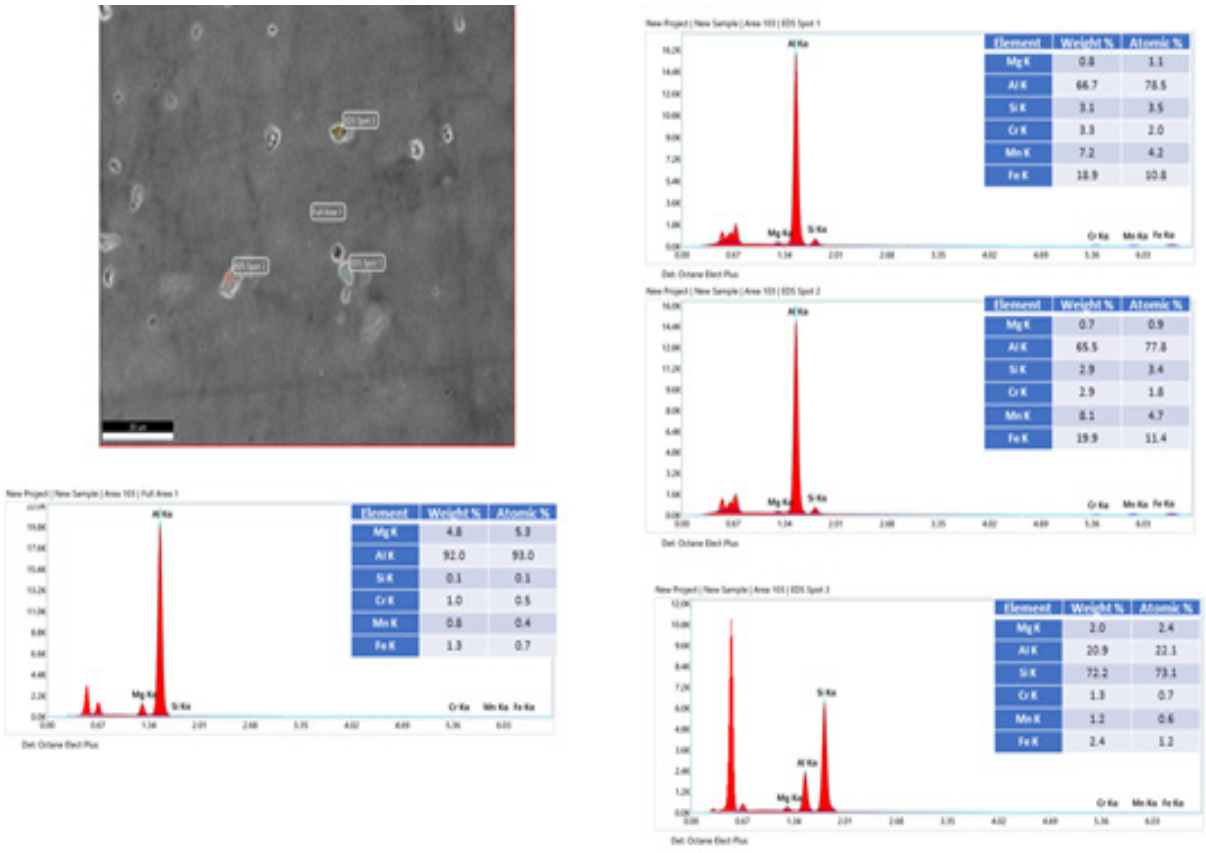


Figure 5. AA5083 alloy - EDS analysis after homogenization at 450°C for 5h.

4(e). MAF with 0.41 strain per pass, shear bands were obtained after 2 cycles, which is shown in Figure 4(g).

Figure 5, shows the EDS analysis of the AA5083 alloy after homogenization. From SEM-EDS analysis, the light-colored particle is Fe and Mn-rich particle and it is suggested to be Al_6(Fe,Mn) Si, and the dark particle consists of a Si-rich particle and is suggested to be an AlMgSi particles[22].

3.3. Mechanical Properties

Microhardness of the alloy in as cast, homogenized, and MAF process with 0.31 and 0.41 strain per pass is shown in Figure 6. Hardness of the alloy in as-cast condition was found to be 73±2.4 HV and after homogenization, hardness slightly increased to 78±3.1 HV. MAF with 0.31 strain per pass, after 1st cycle hardness of the material, is 118±5.1 HV. It increased by 51% compared to the homogenized condition. After 2nd and 3rd cycles, hardness of the material was found to be 123±3.8 HV and 131±3.7 HV respectively. After 1st cycle, the hardness was increased slightly after 2nd and 3rd cycle. After 3rd cycle, hardness of the alloy was increased by 68% compared to the homogenized state. MAF with 0.41 strain per pass, after

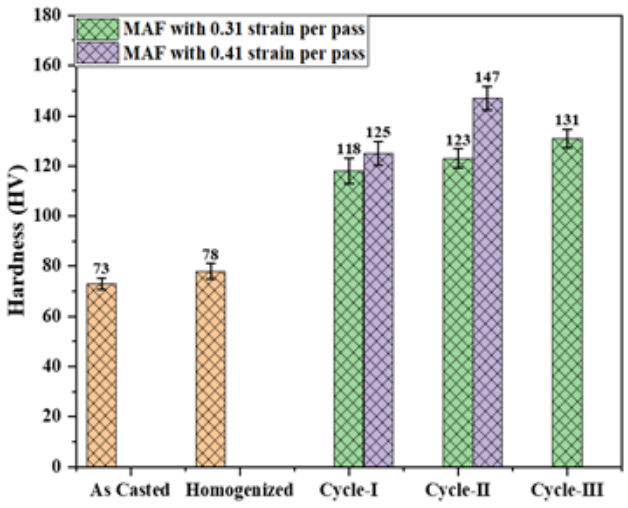


Figure 6. Hardness of the AA5083 alloy subjected to the MAF process.

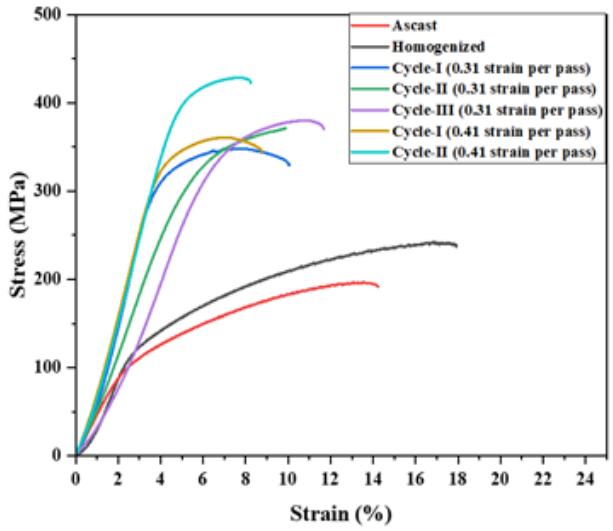


Figure 7. Stress-Strain diagram of AA5083 alloy subjected to different MAF passes.

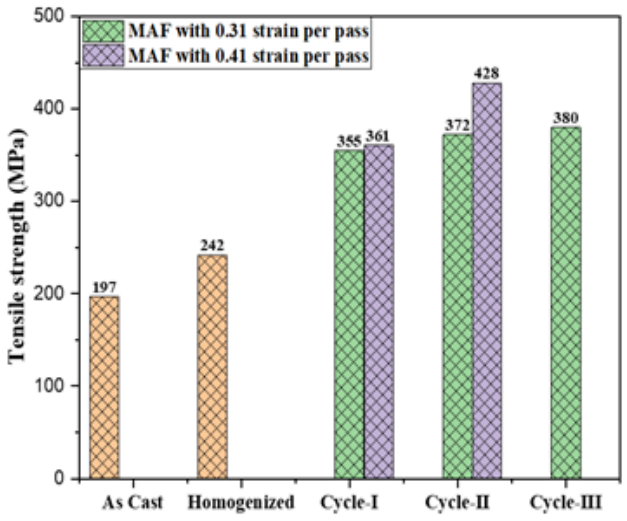


Figure 8. Tensile strength of the AA5083 alloy in as cast, homogenized, and MAF process with different strains per pass.

1st cycle, hardness of the alloy increased by almost 60% compared to the homogenized state and was found to be 125±4.8 HV. After 2nd cycle hardness increased to 147±4.7 HV by almost 88% compared to the homogenized state. Increase in the hardness is attributed to the intensive strain hardening and grain refinement[23].

Stress strain diagram of the AA5083 alloy in different conditions is shown in Figure 7. It is observed that improvement in the mechanical properties with the MAF deformation. Better mechanical properties (tensile strength) with negligible loss in elongation are obtained with 0.41 strain per pass compared to the 0.31 strain per pass.

Tensile strength of the AA5083 alloy under as cast, homogenized, and MAF processed AA5083 alloy with 0.31 and 0.41 strain per pass are shown in Figure 8. MAF processed material shows great improvement in the strength of the material. In as-cast condition, the tensile strength of the alloys showed 197 MPa. After homogenization, the strength of the material was slightly improved and found to be 242 MPa. Tensile strength of the MAF sample with 0.31 strain per pass, after 1st cycle, is greatly improved to 355 MPa. After 2nd and 3rd cycles, the strength of the material increased slightly compared to the first pass. Tensile strength after the 2nd and 3rd cycles were 372 MPa and 380 MPa, respectively. Tensile strength after 1st cycle of MAF with 0.41 strain per pass was 360 MPa. After 2nd cycle, strength improved greatly compared to the 1st cycle and was found to be 428 MPa. After the first cycle of MAF with a strain of 0.31 per pass, the tensile strength of the material was found to have increased by nearly 47% in comparison to its homogenized state, which is attributed to strain hardening and grain refinement. Following the second and third cycles of

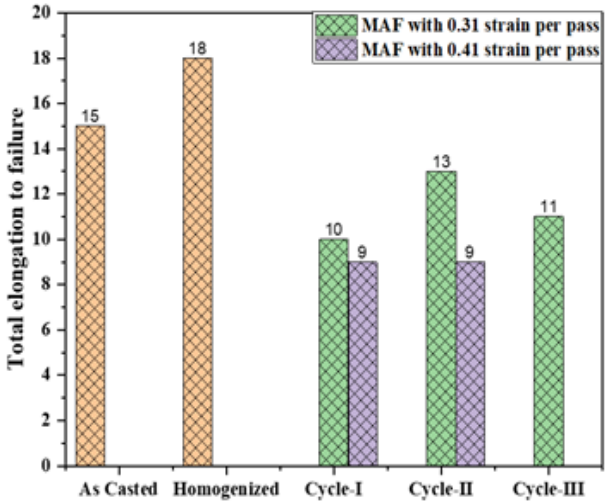


Figure 9. Elongation of the AA5083 alloy, in as cast, homogenized, and MAF process with different strains per pass.

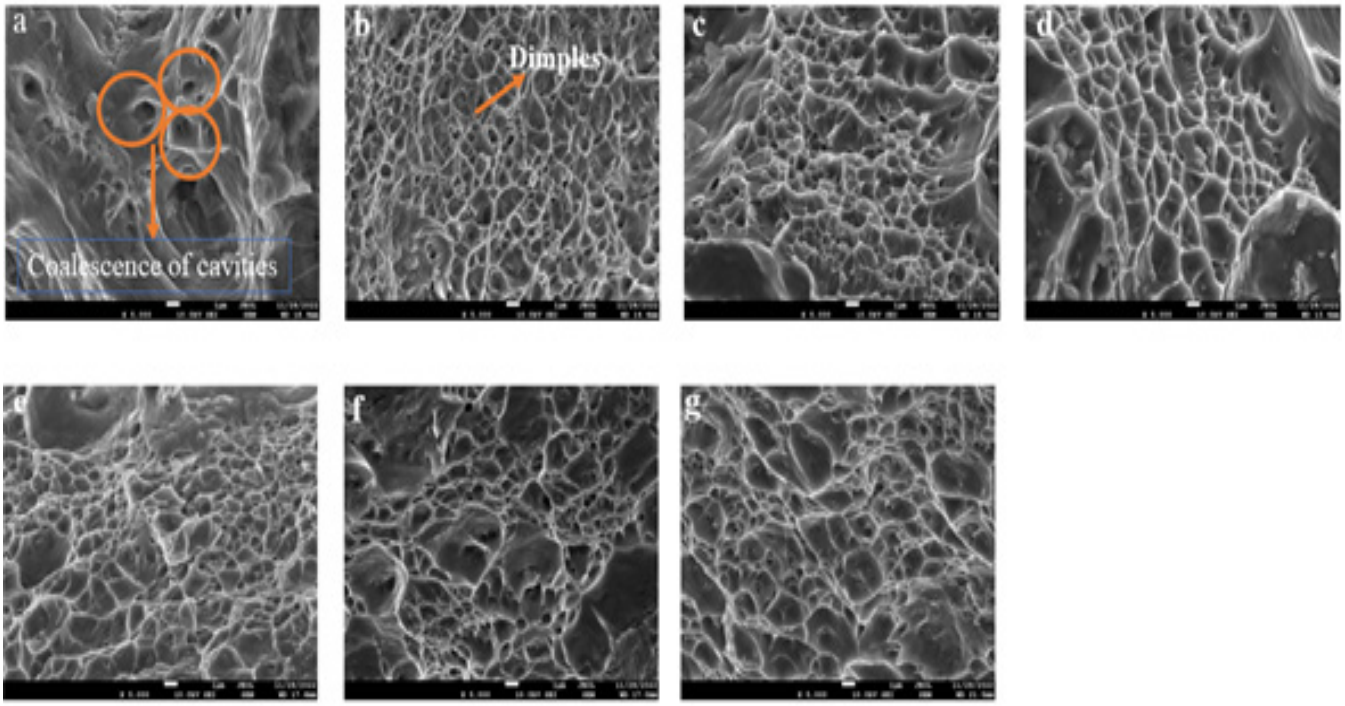


Figure 10. Fractography images of AA5083 alloy **(a)** as cast, **(b)** homogenized, **(c)** I cycle (0.31 strain per pass), **(d)** II cycle (0.31 strain per pass), **(e)** III cycle (0.31 strain per pass), **(f)** I cycle (0.41 strain per pass), **(g)** II cycle (0.41 strain per pass).

MAF, tensile strength was observed to remain relatively constant with a strain of 0.31 per pass. Tensile strength of the AA5083 alloy processed by MAF with 0.41 strain per pass, after 1st cycle is almost equal to 1st cycle with 0.31 strain per pass. After 2nd cycle, the tensile strength of the material increased by almost 77% compared to the homogenized condition and it is attributed to the intense strain hardening and grain refinement.

Elongation of the material in as cast, homogenized, and MAF process with 0.31 and 0.41 strain per pass is shown in Figure 9. In as cast condition elongation of the material was found to be 15%. After homogenization, the elongation of the material slightly increased to 18%. After the first cycle of MAF with a strain of 0.31 per pass, the elongation of the material decreased by 47% compared to its homogenized state and was observed to be 10%. For the next two cycles, the elongation of the material remained at 12% and 11%, respectively. The material's elongation after the first cycle of MAF with a 0.41 strain per pass was reduced by 51%, which is almost near to the first cycle with a 0.31 strain per pass. After the second cycle, the material's elongation remained constant at 9%.

4.0 Fractography

For the fractography analysis, tensile fractured samples of AA5083 alloy subjected to different processes is shown in Figure 10 (a-g). The fracture of the AA5083 alloy was due to the nucleation, growth, and coalescence of the cavities. Figure 10 (a,b) show the fracture surfaces of as cast and homogenized surfaces. Large sized dimples were presented in the as cast and homogenized sample which is due to coarse grain structure. Large cavities were present in throughout the sample in as cast condition due to the coarse grain structure. With increase in the strain dimple size was reduced. Fractography of MAF sample with 0.31 strain per pass shown in Figure 10 (c,d,e). MAF with 0.41 strain per pass shown in Figure 10 (f,g). Dimple size was reduced due to grain refinement[24].

5.0 Conclusions

Work was undertaken in order to evaluate the effect of strain per pass 0.31 and 0.41 in MAF process without

changing the die dimension. The main conclusions derived from this study are as follows

Microstructural and mechanical properties of the AA5083 alloy processed by MAF with 0.41 strain per pass showed better properties compared to the 0.31 strain per pass.

1. Hardness of the material improved greatly after 2nd cycle with 0.41 strain per pass compared to 0.31 strain per pass.
2. Maximum tensile strength of 428 MPa was achieved after two cycles with 0.36 strain per pass compared to 0.31 strain per pass where 380 MPa was achieved after three cycles.
3. Grain size of the material was greatly refined with 0.41 strain per pass and found to be 125 μm.

6.0 References

1. Wang M, Jia P, Lv D, Geng H. Study on the microstructure and liquid-solid correlation of Al-Mg alloys. Phys Chem Liquids. 2016; 54:507-14. https://doi.org/10.1080/00319104.2015.1121784
2. Goswami R, Spanos G, Pao PS, Holtz RL. Microstructural evolution and stress corrosion cracking behavior of Al-5083. Metall Mater Trans A Phys Metall Mater Sci. 2011; 42:348-355. https://doi.org/10.1007/s11661-010-0262-y
3. Searles JL, Gouma PI and RG. Buchheit. Stress corrosion cracking of sensitized AA5083 (Al-4.5Mg-1.0Mn). Materials Science Forum. 2002; 396-402:1437-1442. https://doi.org/10.4028/www.scientific.net/MSF.396-402.1437
4. Jones RH, Baer DR, Danielson MJ, Vetrano JS. Role of Mg in the stress corrosion cracking of an Al-Mg alloy. Metall and Mater Trans A. 2001; 32:1699-711. https://doi.org/10.1007/s11661-001-0148-0
5. Vinogradov A, Estrin Y. Progress in Materials Science Analytical and numerical approaches to modelling severe plastic deformation. Prog Mater Sci. 2018; 95:172-242. https://doi.org/10.1016/j.pmatsci.2018.02.001
6. Manjunath GK, Preetham Kumar GV, Udaya Bhat K. Tensile Properties and Tensile Fracture Characteristics of Cast Al-Zn-Mg Alloys Processed by Equal Channel Angular Pressing. Trans Indian Inst Met. 2017; 70:833-42. https://doi.org/10.1007/s12666-017-1067-0
7. Manjunath GK, Udaya Bhat K and Preetham Kumar GV. Microstructure Evolution in Cast Al Zn-Mg Alloys Processed by Equal Channel Angular Pressing. Metallogr Microstruct Anal. (2018); 7:77-87. https://doi.org/10.1007/s13632-017-0412-3
8. Ibrahim M., El A. The influence of ECAP and HPT processing on the microstructure evolution, mechanical properties and tribology characteristics of an Al6061 alloy. Integr Med Res. 2020; 9:12525-46. https://doi.org/10.1016/j.jmrt.2020.08.099
9. Sitdikov O, Avtokratova E, Markushev M. Development of Ultrafine Grain Structure in an Al-Mg-Mn-Sc-Zr Alloy during High-Temperature Multidirectional Isothermal Forging. Met Mater Inter. 2021; 27:2743-55. https://doi.org/10.1007/s12540-020-00842-2
10. Sheikh H, Paimozd E. Effect of Hot Accumulative Roll Bonding Process on the Mechanical Properties of AA5083. Open J Met. 2011; 01:12-5. https://doi.org/10.4236/ojmetal.2011.11002
11. Anjan BN, Preetham Kumar GV. Wear Behaviour of ZA27-Based Composite Reinforced with 5 wt% of SiC Particles and Processed by Multi-directional Forging. Trans Indian Instit Met. 2019; 72:1621-5. https://doi.org/10.1007/s12666-019-01705-0
12. Kumara B, Preetham Kumar GV. Influence of Multi-directional Room-Temperature Forging Process on Microstructure and Mechanical Behaviour of Eutectic Al-12Si Alloy. Metallogr Microstruct Anal. 2022; 11:175-82. https://doi.org/10.1007/s13632-022-00836-z
13. Muralidharan S, Iqbal UM. Analysis of Multi-angular Twist Channel Extrusion Technique for Processing AA2024 Aluminium Alloy. Met Mater Inter. 2022; 29:515-35. https://doi.org/10.1007/s12540-022-01221-9
14. Sharath PC. Multi directional forging: An advanced deforming technique for severe plastic deformation. Advanced Welding and Deforming, Elsevier. 2021; pp. 529-56. https://doi.org/10.1016/B978-0-12-822049-8.00017-7
15. Sitdikov O, Sakai T, Goloborodko A, Miura H. Grain fragmentation in a coarse-grained 7475 Al alloy during hot deformation. Scr Mater. 2004; 51:175-9. https://doi.org/10.1016/j.scriptamat.2004.02.034
16. Nakashima K, Horita Z, Nemoto M, Langdon TG. Influence of channel angle on the development of ultrafine grains in equal-channel angular pressing. Acta Mater. 1998; 46: 1589-99. https://doi.org/10.1016/S1359-6454(97)00355-8
17. Sitdikov O, Sakai T, Goloborodko A, Miura H, Kaibyshev R. Effect of Pass Strain on Grain Refinement in 7475 Al Alloy during Hot Multidirectional Forging. Mater Trans. 2004; 45:2232-8. https://doi.org/10.2320/matertrans.45.2232

18. Estrin Y, Vinogradov A. Extreme grain refinement by severe plastic deformation: A wealth of challenging science. Acta Mater. 2013; 61:782-817. https://doi.org/10.1016/j.actamat.2012.10.038
19. Totten GE, MacKenzie DS. (Eds.). Handbook of Aluminum: Volume 2: Alloy Production and Materials Manufacturing (1st ed.). CRC Press. 2013.
20. Howeyze M, Eivani AR, Arabi H, Jafarian HR. Effects of deformation routes on the evolution of microstructure, texture and tensile properties of AA5052 aluminum alloy. Mater Sci Eng A. 2018; 732:120-8. https://doi.org/10.1016/j.msea.2018.06.081
21. Gu H, Bhatta L, Gao H, Li Z, C Kong, Yu H. Effect of cryorolling on the microstructure and high-temperature mechanical properties of AA5083 sheets. Mater Sci Eng A. 2022; 843:143141. https://doi.org/10.1016/j.msea.2022.143141
22. Engler O, Miller-Jupp S. Control of second-phase particles in the Al-Mg-Mn alloy AA 5083. J Alloys Compd. 2016; 689:998-1010. https://doi.org/10.1016/j.jallcom.2016.08.070
23. Babaei A, Jafarzadeh H, Mazloumbashiri H. Processing ultrafine grained non-circular cross-section profiles via severe plastic deformation. Proceedings of the Institution of Mechanical Engineers. Part L: Journal of Materials: Design and Applications. 2021; 235:572-80. https://doi.org/10.1177/1464420720972737
24. Gu H, Bhatta L, Gao H, Li Z, Kong C, Yu H. Effect of cryorolling on the microstructure and high-temperature mechanical properties of AA5083 sheets. Mater Sci Eng: A. 2022; 843:143141. https://doi.org/10.1016/j.msea.2022.143141